# The Dijet Mass Spectrum and a Search for Quark Compositeness in $\bar{p}p$ Collisions at $\sqrt{s} = 1.8$ TeV

The DØ Collaboration *
*Fermi National Accelerator Laboratory, Batavia, Illinois 60510*
(June 15, 1999)

## Abstract

Using the DØ detector at the 1.8 TeV $\bar{p}p$ Fermilab Tevatron collider, we have measured the inclusive dijet mass spectrum in the central pseudorapidity region $|\eta_{\rm jet}| < 1.0$ for dijet masses greater than 200 GeV/$c^2$. We have also measured the ratio of spectra $\sigma(|\eta_{\rm jet}| < 0.5)/\sigma(0.5 < |\eta_{\rm jet}| < 1.0)$. The order $\alpha_s^3$ QCD predictions are in good agreement with the data and we rule out models of quark compositeness with a contact interaction scale $< 2.4$ TeV at the 95% confidence level.

*Submitted to the *International Europhysics Conference* on *High Energy Physics*, *EPS-HEP99*, 15 – 21 July, 1999, Tampere, Finland.

High transverse energy ($E_T$) jet production at a center of mass energy of 1.8 TeV probes the structure of the proton down to a distance scale of $10^{-4}$ fm. A measurement of the dijet mass spectrum can be used to verify the predictions of quantum chromodynamics (QCD) for parton-parton scattering and to constrain the parton distribution functions (pdf) of the proton. Additionally, new physics such as quark compositeness [1] would be revealed by an excess of events in the dijet mass ($M$) spectrum at high masses with respect to the predictions of QCD. A previous analysis by the CDF collaboration of the inclusive jet cross section [2] reported an excess of jet production at high $E_T$. More recent analyses of the dijet angular distribution by DØ [3] and CDF [4] have excluded at the 95% confidence level models of quark compositeness in which the contact interaction scale is below 2 TeV. Most recently, an analysis of the inclusive jet cross section by DØ [5] shows good agreement between the theory and data. This paper presents a new improved measurement by DØ of the inclusive dijet mass ($M$) spectrum (uncertainty reduced by a factor of four at $M = 200$ GeV/$c^2$ relative to the previous CDF measurement [6]) and improved limits on the contact interaction scale.

The outgoing partons from the parton-parton scattering process hadronize to form jets of particles. These jets were identified in the DØ detector [7] using uranium/liquid-argon calorimeters which cover a pseudorapidity range of $|\eta| \leq 4.1$ ($\eta = -\ln[\tan(\theta/2)]$, where $\theta$ is the polar angle).

Events with at least one inelastic interaction during a beam crossing were identified using scintillator hodoscopes, and the primary event vertex was determined using tracks reconstructed in the central tracking system. Event selection occurred in two stages. First, a minimum transverse energy was required in a region ($\Delta\eta \times \Delta\phi = 0.8 \times 1.6$) of the calorimeter. Jet candidates were then reconstructed online with a cone algorithm of opening angle $\mathcal{R} = 0.7$ in $\eta$–$\phi$ space ($\phi$ is the azimuthal angle), and the event was recorded if any jet $E_T$ exceeded a specified threshold. During the 1994–95 run, the thresholds were 30, 50, 85, and 115 GeV, with integrated luminosities of 0.353±0.027, 4.69±0.37, 54.7±3.4, and 91.9±5.6 pb$^{-1}$, respectively [8]. The luminosities of the 30 and 50 GeV triggers were determined by matching their dijet cross sections to that measured for the 85 GeV trigger. This resulted in an additional uncertainty of 4.9% in the luminosities of the 30 and 50 GeV triggers.

Jets were reconstructed offline using an iterative jet cone algorithm with $\mathcal{R} = 0.7$ [9]. Jet $E_T$ is defined as the sum of the $E_T$ in each cell within the cone. The jet was centered on the $E_T$-weighted pseudorapidity and azimuth of the jet. The jet $E_T$ and direction were then recalculated until the cone direction was stable.

A significant fraction of the data was taken at high instantaneous luminosity, which resulted in more than one $\bar{p}p$ interaction in a beam crossing leading to an ambiguity in selecting the primary event vertex. After event reconstruction, the two vertices with the largest track multiplicity were retained. The quantity $S_T = |\Sigma \vec{E}_T^{\rm jet}|$ was calculated for both vertices, and the vertex with the smaller $S_T$ was selected. The uncertainty on the mass spectrum due to the choice of vertex was 2%. The vertex was required to be within 50 cm of the detector center. This cutoff was $90 \pm 1$% efficient, independent of $M$.

Backgrounds from noise, cosmic rays, and accelerator losses were reduced to an insignificant level by applying jet quality criteria. For an event to be accepted, the two leading-$E_T$ jets were required to satisfy these criteria. Contamination from backgrounds was $< 2$% based on Monte Carlo simulations and visual inspection of events with high mass. The over-

all jet selection efficiency for the mass spectrum for $|\eta| \leq 1.0$ was measured as a function of $M$, giving $93 \pm 1\%$ ($89 \pm 1\%$) at 209 (873) GeV/$c^2$.

The transverse energy of each jet was corrected for the underlying event, additional interactions, calorimeter noise, the fraction of particle energy that showered hadronically outside of the cone, and for the hadronic response [10]. At $\eta = 0$, the mean total jet energy correction was 16% (12%) at 100 GeV (400 GeV); the correction uncertainty was less than 2.5% of the jet $E_T$.

For each event that passed the criteria, the dijet mass, $M$, was calculated, assuming that the jets are massless, using $M^2 = 2E_T^{\rm jet1}E_T^{\rm jet2}[\cosh(\Delta\eta) - \cos(\Delta\phi)]$.

The steeply falling dijet mass spectrum is distorted by jet energy resolution (and to a negligible extent by $\eta$ resolution). The dijet mass resolution was calculated using the measured single-jet resolutions and the PYTHIA [11] Monte Carlo event generator. This resolution depends on the $E_T$ and $\eta$ distributions of the two leading $E_T$ jets in each event and is $6.4 \pm 0.7\%$ ($3.8 \pm 0.8\%$) at 200 (1000) GeV/$c^2$. The observed mass spectrum was corrected with an ansatz function $F(M') = BM'^{-\alpha}[1-(M'/\sqrt{s})]^{-\beta}$ convoluted with the mass resolutions, to obtain the smeared ansatz $f(M) = \int_0^\infty F(M')\rho(M'-M,M')dM'$ (where $\rho$ is the mass resolution), such that the number of events in any given mass bin $i$ is given by integrating $f$ over that bin. The data were then fitted using a binned maximum likelihood method and the MINUIT [12] package to determine the values of $B$, $\alpha$, and $\beta$ ($\chi^2 = 10.8$ for 12 degrees of freedom). The unsmearing correction for each mass bin is then given by $C_i = \int F dM / \int f dM$ ($C_i = 0.96$ (0.92) at 209 (873) GeV/$c^2$).

The dijet mass spectrum was calculated using $\kappa \equiv d^3\sigma/dMd\eta_1 d\eta_2 = (N_i C_i)/(\mathcal{L}_i \epsilon \Delta M \Delta\eta_1 \Delta\eta_2)$, where $N_i$ is the number of events, $\mathcal{L}_i$ is the luminosity, $\epsilon$ is the efficiency of the vertex selection and jet quality cuts, $\Delta M$ is the width of the mass bin, and $\Delta\eta_{1,2}$ is the width of the $\eta$ bin for jets 1 and 2. The spectrum was calculated for the pseudorapidity range $|\eta_{\rm jet}| < 1.0$ (both jets are required to satisfy the $\eta$ requirement), in mass ranges starting at 200, 270, 350, and 550 GeV/$c^2$, corresponding to jet $E_T$ thresholds of 30, 50, 85, and 115 GeV.

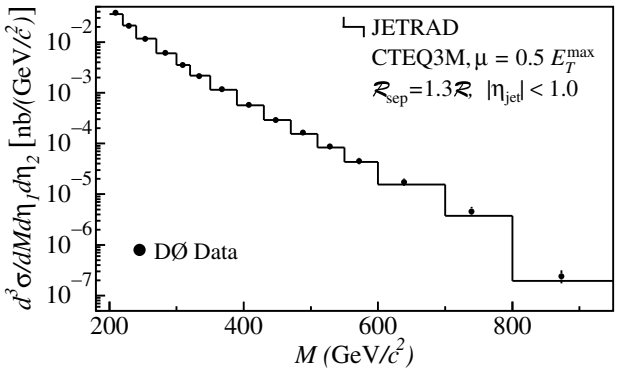


FIG. 1. $d^3\sigma/dMd\eta_1 d\eta_2$ for $|\eta_{\rm jet}| < 1.0$. The DØ data are shown by the solid circles, with error bars representing the $\pm 1\sigma$ statistical and systematic uncertainties added in quadrature (in most cases smaller than the symbol). The histogram represents the JETRAD prediction.

The cross section for the mass spectrum is plotted in Fig. 1, and given in Table I. The data are plotted at the mass-weighted average of the fit function for each bin

TABLE I. Dijet cross section for $|\eta_{\rm jet}| < 1.0$, and the ratio $\kappa(|\eta_{\rm jet}| < 0.5)/\kappa(0.5 < |\eta_{\rm jet}| < 1.0)$. High (low) systematic uncertainties are the sum in quadrature of the uncertainties from the $\pm 1\sigma$ variations in the energy calibration, the unsmearing, the vertex corrections, luminosity matching, jet selection, and the uncertainty in the luminosity.

| Mass Bin (GeV/$c^2$) | | | | $d^3\sigma/dMd\eta_1 d\eta_2$ | | | Ratio of Mass Spectra |
|---|---|---|---|---|---|---|---|
| Bin | Min. | Max. | Weighted Center | $\pm$ Stat. Error (nb) | Syst. Low (%) | Syst. High (%) | $\kappa(\lvert\eta_{\rm jet}\rvert < 0.5)/\kappa(0.5 < \lvert\eta_{\rm jet}\rvert < 1.0)$ ($\pm$ stat. error $\pm$ syst. errror) |
| 1 | 200 | 220 | 209.1 | $(3.78 \pm 0.12)\times 10^{-2}$ | $-11.4$ | $+11.8$ | $0.613 \pm 0.039 \pm 0.037$ |
| 2 | 220 | 240 | 229.2 | $(2.10 \pm 0.09)\times 10^{-2}$ | $-11.3$ | $+11.6$ | $0.614 \pm 0.050 \pm 0.030$ |
| 3 | 240 | 270 | 253.3 | $(1.16 \pm 0.06)\times 10^{-2}$ | $-11.5$ | $+11.7$ | $0.570 \pm 0.051 \pm 0.029$ |
| 4 | 270 | 300 | 283.4 | $(6.18 \pm 0.11)\times 10^{-3}$ | $-11.5$ | $+12.0$ | $0.568 \pm 0.030 \pm 0.027$ |
| 5 | 300 | 320 | 309.3 | $(3.55 \pm 0.11)\times 10^{-3}$ | $-11.5$ | $+12.1$ | $0.610 \pm 0.034 \pm 0.050$ |
| 6 | 320 | 350 | 333.6 | $(2.12 \pm 0.07)\times 10^{-3}$ | $-11.9$ | $+12.3$ | $0.705 \pm 0.044 \pm 0.058$ |
| 7 | 350 | 390 | 367.6 | $(1.18 \pm 0.01)\times 10^{-3}$ | $-11.1$ | $+11.6$ | $0.672 \pm 0.020 \pm 0.032$ |
| 8 | 390 | 430 | 407.8 | $(5.84 \pm 0.09)\times 10^{-4}$ | $-11.5$ | $+12.2$ | $0.593 \pm 0.022 \pm 0.030$ |
| 9 | 430 | 470 | 447.9 | $(2.89 \pm 0.06)\times 10^{-4}$ | $-11.9$ | $+12.9$ | $0.708 \pm 0.036 \pm 0.037$ |
| 10 | 470 | 510 | 488.0 | $(1.64 \pm 0.05)\times 10^{-4}$ | $-12.4$ | $+13.5$ | $0.690 \pm 0.046 \pm 0.036$ |
| 11 | 510 | 550 | 528.0 | $(8.74 \pm 0.34)\times 10^{-5}$ | $-12.8$ | $+14.3$ | $0.620 \pm 0.058 \pm 0.033$ |
| 12 | 550 | 600 | 572.0 | $(4.49 \pm 0.17)\times 10^{-5}$ | $-13.5$ | $+15.3$ | $0.634 \pm 0.065 \pm 0.033$ |
| 13 | 600 | 700 | 638.9 | $(1.73 \pm 0.07)\times 10^{-5}$ | $-14.9$ | $+17.2$ | $0.647 \pm 0.074 \pm 0.034$ |
| 14 | 700 | 800 | 739.2 | $(4.58 \pm 0.38)\times 10^{-6}$ | $-17.6$ | $+20.8$ | $0.608 \pm 0.141 \pm 0.035$ |
| 15 | 800 | 1400 | 873.2 | $(2.39 \pm 0.35)\times 10^{-7}$ | $-23.2$ | $+28.9$ | $0.705 \pm 0.246 \pm 0.046$ |

($\int MFdM/\int FdM$). The systematic uncertainties are dominated by the uncertainties due to the jet energy scale, which are 7% (30%) for the 209 (873) GeV/$c^2$ mass bins. The other uncertainties are due to the luminosity measurement (6.1%); luminosity matching at low mass (4.9%); the unsmearing correction, 0.5% (3%) at 209 (873) GeV/$c^2$; the vertex cut (1%); and the jet selection cuts (1%). The total systematic uncertainty is given by the sum of the individual uncertainties in quadrature. The bin-to-bin correlations of the uncertainties are shown in Fig. 2 [13].

The histogram in Fig. 1 is a prediction for the inclusive dijet mass spectrum from the next-to-leading (NLO) parton level event generator JETRAD [14]. The NLO calculation requires specification of the renormalization and factorization scales ($\mu = 0.5E_T^{\rm max}$ where $E_T^{\rm max}$ is the maximum jet $E_T$ in the generated event), pdf (CTEQ3M [15]), and parton clustering algorithm. Two partons are combined if they are within $\mathcal{R}_{\rm sep} = 1.3\mathcal{R}$, as motivated by the separation of jets in the data [9]. Choosing an alternative pdf (CTEQ4M [15], CTEQ4HJ [15], or MRS(A′) [16]) alters the prediction by as much as 25%, and varying $\mu$ in the range $0.25E_T^{\rm max}$ to $2E_T^{\rm max}$ alters the normalization by up to 30% with some $M$ dependence. The CTEQ3M and MRS(A′) pdf's are fits to collider and fixed target data sets published before 1994. CTEQ4M updates these fits using data published before 1996, and CTEQ4HJ adjusts the gluon distributions to fit the CDF inclusive jet cross section measurement [2].

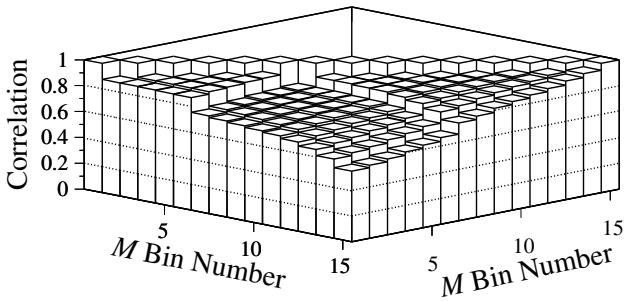


FIG. 2. The correlations between systematic uncertainties in bins of dijet mass (see Table I) for $|\eta_{\rm jet}| < 1.0$. The correlations are calculated using the average systematic uncertainty. The discontinuities arise from the uncorrelated errors (adjacent to correlations of 1.0) and luminosity matching.

Figure 3 shows the ratio (Data−Theory)/Theory for the JETRAD prediction using CTEQ3M with $\mu = 0.5E_T^{\rm max}$. Given the experimental and theoretical uncertainties, the predictions can be regarded as in good agreement with the data. The data are also in agreement within the given uncertainties with the cross section measured by CDF [6].

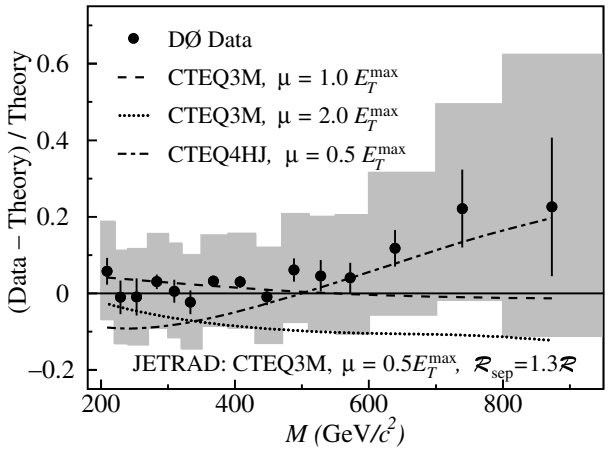


FIG. 3. The difference between the data and the prediction (JETRAD) divided by the prediction for $|\eta_{\rm jet}| < 1.0$. The solid circles represent the comparison to the calculation using CTEQ3M with $\mu = 0.5E_T^{\rm max}$. The shaded region represents the $\pm 1\sigma$ systematic uncertainties. The effects of changing the renormalization scale and choosing a different pdf are also shown (each curve shows the difference between the alternative prediction and the standard prediction).

In Table II, we show the $\chi^2$ resulting from a fit of theory to our data, using the full correlation matrix between different mass bins. The choice of pdf and renormalization scale is varied; all choices give reasonable probability.

The ratio $\kappa(|\eta_{\rm jet}| < 0.5)/\kappa(0.5 < |\eta_{\rm jet}| < 1.0)$, given in Fig. 4 and Table I, exploits the high correlation between uncertainties in the measurement of the dijet mass spectrum. The resulting cancelation of uncertainties leads to a systematic error of less than 8% for all $M$. The uncertainty in the theoretical prediction of this ratio is less than 3% due to the choice of pdf, and 6% from the choice of renormalization and factorization scale (excluding $\mu = 0.25E_T^{\rm max}$). The $\chi^2$ values are shown in Table II. The predictions are in good agreement with the data, except for $\mu = 0.25E_T^{\rm max}$ which is excluded by the data.

TABLE II. $\chi^2$ values calculated for various theoretical predictions for the dijet mass spectrum with $|\eta_{\rm jet}| < 1.0$, and for the ratio of cross sections (15 degrees of freedom).

| pdf | D | Mass Spectrum | | Ratio | |
|---|---|---|---|---|---|
| | where $\mu = DE_T^{\rm max}$ | $\chi^2$ | Prob. | $\chi^2$ | Prob. |
| CTEQ3M | 0.25 | 12.2 | 0.66 | 40.5 | 0.00 |
| CTEQ3M | 0.50 | 5.0 | 0.99 | 15.9 | 0.39 |
| CTEQ3M | 0.75 | 5.3 | 0.99 | 14.7 | 0.48 |
| CTEQ3M | 1.00 | 5.4 | 0.99 | 14.3 | 0.51 |
| CTEQ3M | 2.00 | 4.2 | 1.00 | 13.7 | 0.55 |
| CTEQ4M | 0.50 | 4.9 | 0.99 | 15.7 | 0.40 |
| CTEQ4HJ | 0.50 | 5.0 | 0.99 | 16.0 | 0.38 |
| MRS(A′) | 0.50 | 6.3 | 0.97 | 16.3 | 0.36 |

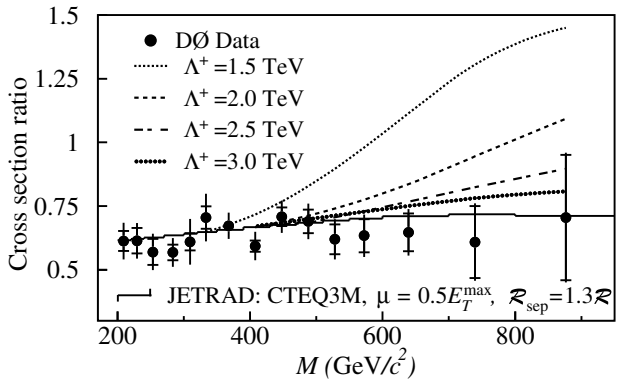


FIG. 4. The ratio of cross sections for $|\eta_{\rm jet}| < 0.5$ and $0.5 < |\eta_{\rm jet}| < 1.0$ for data (solid circles) and theory (various lines). The error bars show the statistical and systematic uncertainties added in quadrature, and the crossbar shows the size of the statistical error.

The ratio of the mass spectra can be used to place limits on quark compositeness. A mass scale $\Lambda$ characterizes both the strength of the quark-substructure coupling and the physical size of the composite state. Limits are set assuming that $\Lambda \gg \sqrt{\hat{s}}$ (where $\sqrt{\hat{s}}$ is the center of mass energy of the colliding partons), such that quarks appear to be point-like. Hence, the substructure coupling can be approximated by a four-Fermi contact interaction giving rise to an effective Lagrangian [1] $\mathcal{L} = A(2\pi/\Lambda^2)(\bar{q}_L\gamma^\mu q_L)(\bar{q}_L\gamma_\mu q_L)$, where $A = \pm 1$, and $q_L$ represents left-handed quarks. Limits are presented for the case where all quarks are composite, showing both constructive interference ($\Lambda^-$ for $A = -1$) and destructive interference ($\Lambda^+$ for $A = +1$). Currently there are no NLO compositeness calculations available; therefore, the PYTHIA event generator is used to simulate the effect of compositeness. The ratio of these LO predictions with compositeness, to the LO with no compositeness, is used to scale the JETRAD NLO prediction, as shown in Fig. 4.

We employ a Bayesian technique [17] to obtain from our data a limit on the scale of compositeness. Motivated by the form of the Lagrangian, a uniform prior is assumed in

$\xi = 1/\Lambda^2$, and a Gaussian likelihood function $P \propto e^{-\chi^2/2}$ is used. The 95% confidence limit in $\Lambda$ is determined by requiring that $\int_0^\xi P(\xi')d\xi' = 0.95$. Since the ratio at NLO is sensitive to the choice of $\mu$ and pdf, each possible choice is treated as a different theory. The most conservative (CTEQ3M, $\mu = E_T^{\max}$) lower limits on the mass scale at the 95% confidence level are found to be $\Lambda^+ > 2.7$ TeV and $\Lambda^- > 2.4$ TeV. These limits are incompatible with the suggestion of a compositeness scale $\Lambda$ in the 1.5 to 1.8 TeV range found from earlier measurements [2] of the high $E_T$ jet inclusive cross section.

In conclusion, we have measured the cross section for the inclusive dijet mass spectrum for $|\eta_{\rm jet}| < 1.0$ with $M > 200$ GeV/$c^2$, and the ratio of cross sections for $|\eta_{\rm jet}| < 0.5$ and $0.5 < |\eta_{\rm jet}| < 1.0$, as a function of dijet mass. The data distributions are in good agreement with NLO QCD predictions. Models of quark compositeness with a contact interaction scale of less than 2.4 TeV are excluded at the 95% confidence level.

We thank the Fermilab and collaborating institution staffs for contributions to this work and acknowledge support from the Department of Energy and National Science Foundation (USA), Commissariat à L'Energie Atomique (France), Ministry for Science and Technology and Ministry for Atomic Energy (Russia), CAPES and CNPq (Brazil), Departments of Atomic Energy and Science and Education (India), Colciencias (Colombia), CONACyT (Mexico), Ministry of Education and KOSEF (Korea), and CONICET and UBACyT (Argentina).

# REFERENCES


[1] E. Eichten, K. Lane, and M.E. Peskin, Phys. Rev. Lett. **50**, 811 (1983); E. Eichten, I. Hinchcliffe, K. Lane, and C. Quigg, Rev. Mod. Phys. **56**, 579 (1984), Addendum — ibid. **58** 1065 (1986); K. Lane, hep-ph/9605257 (1996).

[2] CDF Collaboration, F. Abe *et al.*, Phys. Rev. Lett. **77**, 438 (1996).

[3] DØ Collaboration, B. Abbott *et al.*, Phys. Rev. Lett. **80**, 666 (1998)

[4] CDF Collaboration, F. Abe *et al.*, Phys. Rev. Lett. **77**, 5336 (1996); erratum — ibid. **78**, 4307 (1997).

[5] DØ Collaboration, B. Abbott *et al.*, hep-ex/9807018, submitted to Phys. Rev. Lett.

[6] CDF Collaboration, F. Abe *et al.*, Phys. Rev. D **48**, 998 (1993).

[7] DØ Collaboration, S. Abachi *et al.*, Nucl. Instr. Meth. Phys. Res. **A 338**, 185 (1994).

[8] J. Bantly *et al.*, Fermilab-TM-1995, (1997)

[9] B. Abbott *et al.*, Fermilab-Pub-97/242-E.

[10] DØ Collaboration, B. Abbott *et al.*, hep-ex/9805009, submitted to Nucl. Instr. Meth. Phys. Res. **A**.

[11] T. Sjöstrand, Computer Physics Commun. **82**, 74 (1994). We used PYTHIA version 5.7.

[12] F. James, CERN Program Library Entry D506 (unpublished), We used MINUIT version 96.a.

[13] The correlation matrix is available at
`http://www-d0.fnal.gov/~d0qcd/dijet_mass/.`
It will also be available from the AIP E-PAPS service.

[14] W.T. Giele, E.W.N. Glover, and D.A. Kosower, Nucl. Phys. **B403**, 633 (1993). We used JETRAD version 2.0.

[15] CTEQ Collaboration, H.L. Lai *et al.*, Phys. Rev. D **51**, 4763 (1995); CTEQ Collaboration, H.L. Lai *et al.*, Phys. Rev. D **55**, 1280 (1997).

[16] A.D. Martin, R.G. Roberts, and W.J. Stirling, Phys. Lett. **B354**, 155 (1995).

[17] H. Jeffreys, *Theory of Probability* (Clarendon Press, Oxford, 1939, revised 1988), p 94.